



NRC Publications Archive Archives des publications du CNRC

Ab Initio study of ionic liquids by KS-DFT/3D-RISM-KH theory

Malvaldi, Marco; Bruzzone, Samantha; Chiappe, Cinzia; Gusarov, Sergey;
Kovalenko, Andriy

This publication could be one of several versions: author's original, accepted manuscript or the publisher's version. /
La version de cette publication peut être l'une des suivantes : la version prépublication de l'auteur, la version
acceptée du manuscrit ou la version de l'éditeur.

For the publisher's version, please access the DOI link below. / Pour consulter la version de l'éditeur, utilisez le lien
DOI ci-dessous.

Publisher's version / Version de l'éditeur:

<https://doi.org/10.1021/jp810887z>

The Journal of Physical Chemistry B, 113, 11, pp. 3536-3542, 2009-03-19

NRC Publications Record / Notice d'Archives des publications de CNRC:

<https://nrc-publications.canada.ca/eng/view/object/?id=327be92b-01e0-458f-90d2-e166ba7d9f85>

<https://publications-cnrc.canada.ca/fra/voir/objet/?id=327be92b-01e0-458f-90d2-e166ba7d9f85>

Access and use of this website and the material on it are subject to the Terms and Conditions set forth at

<https://nrc-publications.canada.ca/eng/copyright>

READ THESE TERMS AND CONDITIONS CAREFULLY BEFORE USING THIS WEBSITE.

L'accès à ce site Web et l'utilisation de son contenu sont assujettis aux conditions présentées dans le site

<https://publications-cnrc.canada.ca/fra/droits>

LISEZ CES CONDITIONS ATTENTIVEMENT AVANT D'UTILISER CE SITE WEB.

Questions? Contact the NRC Publications Archive team at

PublicationsArchive-ArchivesPublications@nrc-cnrc.gc.ca. If you wish to email the authors directly, please see the
first page of the publication for their contact information.

Vous avez des questions? Nous pouvons vous aider. Pour communiquer directement avec un auteur, consultez la
première page de la revue dans laquelle son article a été publié afin de trouver ses coordonnées. Si vous n'arrivez
pas à les repérer, communiquez avec nous à PublicationsArchive-ArchivesPublications@nrc-cnrc.gc.ca.



Ab Initio Study of Ionic Liquids by KS-DFT/3D-RISM-KH Theory

Marco Malvaldi,^{*,†} Samantha Bruzzone,[‡] Cinzia Chiappe,[†] Sergey Gusarov,[§] and Andriy Kovalenko^{§,||}

Dipartimento di Bioorganica e Biofarmacia, Università di Pisa, Via Bonanno, Pisa, Italy, Dipartimento di Chimica e Chimica Industriale, Università di Pisa, Via Risorgimento 35, Pisa, Italy, Institute for Nanotechnology, National Research Council of Canada, 421 Saskatchewan Drive, Edmonton, Alberta, T6G 2M9 Canada, and Department of Mechanical Engineering, University of Alberta, Edmonton, Alberta, Canada

Received: December 10, 2008; Revised Manuscript Received: January 13, 2009

Properties of molecules solvated in ionic liquids (ILs) are strongly affected by solvent environment. For this reason, to give reliable results, ab initio calculations on solutes in ILs, including ions constituting ionic liquid itself, have to self-consistently account for the change of both electronic and classical solvation structure in ILs. Here, we study the electronic structure of the methyl–methylimidazolium ion in the bulk liquid of [mmim][Cl] by using the self-consistent field coupling of Kohn–Sham density functional theory and three-dimensional molecular theory of solvation (aka 3D-RISM) with the closure approximation of Kovalenko and Hirata. The KS-DFT/3D-RISM-KH method yields the 3D distribution of the IL solvent species around the [mmim] solute, underlying the most important peculiarities of this kind of systems such as the stacking interaction between neighboring cations, and reproduces the enhancement of the dipole moment resulting from the polarization of the cation by the solvent in a very good agreement with the results of an ab initio MD calculation. The KS-DFT/3D-RISM-KH method offers an accurate and computationally efficient procedure to perform ab initio calculations on species solvated in ionic liquids.

1. Introduction

Room-temperature ionic liquids (ILs) is a novel class of organic systems attracting increasing research efforts and utilization in organic synthesis due to their peculiar properties.¹ Because ILs are being used principally as solvents in organic synthesis and other applications such as electrodeposition, investigation of their liquid structure and of their effect on various organic and inorganic solutes becomes a task of primary importance.

In bulk liquid, the solvent environment affects physicochemical characteristics of ILs constituents (NMR chemical shifts,² relaxation times, IR frequencies),⁴ as well as important chemical behavior (acidity of aromatic protons). Therefore, when theoretically studying chemical processes occurring in ionic liquids, it is mandatory to involve a reliable description of solvation environment. This can be achieved, in principle, by a QM/MD approach in which QM treats one selected ion of the ionic liquid and MD handles the solvent effect. However, it is extremely computationally demanding, especially to obtain solvation thermodynamics. Another, simpler approach is QM/MM calculation. However, the MM part cannot represent the solvation structure and thermodynamics in a statistical ensemble average.

An appropriate description of both solvation structure and thermodynamics is provided by statistical-mechanical, molecular theory of solvation, also known as the reference interaction site model (RISM).^{5–9} Its three-dimensional generalization (3D-RISM)^{9–12} properly resolves a 3D spatial map of solvation structure and reliably describes solvation effects for macromolecules with complex geometry and different chemical specificities, such as

hydrogen bonding and/or solvophobic solvation and solvophobic interaction.⁹ An important ingredient of liquid state theory is a closure approximation to the integral equations, as it should properly represent the essential physics of the system.⁸ In particular, the approximation proposed by Kovalenko and Hirata (KH closure)^{9,12} is appropriate for complex liquids, electrolyte solutions, and solid–liquid interfaces containing species with significant total and/or partial charges that are characterized by strong association forces (e.g., hydrogen bonding), and for fluid systems near phase transition lines. Successful predictions of 3D-RISM-KH theory include such complex examples as supramolecular hierarchical self-assembly and conformational stability of organic rosette nanotubes in aqueous electrolyte solution¹³ and different (polar and apolar) solvents,¹⁴ and solvent-controlled formation of conformers with different supramolecular chirality (rosette nanotube “chiomers”).¹⁵

To describe electronic structure in solution, the 3D-RISM-KH theory was coupled in a multiscale method with Kohn–Sham density functional theory (KS-DFT)^{9,12} and with ab initio CASSCF theory.^{9,16} The 3D-RISM-KH theory provides, from the first principles of statistical mechanics, analytical gradients including all the solvation contributions, both electrostatic and nonelectrostatic (such as cavitation, dispersion, and repulsion).¹⁷ This allows one to accurately determine the potential energy surface, optimize molecular geometry in solution, and predict chemical reactions in solution. A crucial advantage of the KS-DFT/3D-RISM-KH method is a first-principle, physical view on electronic structure in solution. With reasonable computational efforts, it allows one to predict the electronic structure and geometry of solvated macromolecules, their thermochemistry, chemical reactions in solution, and solvent in inner spaces of nanostructures such as channels of nanotubes.¹⁸ The self-consistent field KS-DFT/3D-RISM-KH method with analytical

[†] Dipartimento di Bioorganica e Biofarmacia, Università di Pisa.

[‡] Dipartimento di Chimica e Chimica Industriale, Università di Pisa.

[§] National Research Council of Canada.

^{||} University of Alberta.

gradients has been implemented¹⁷ in a development version of the Amsterdam density functional (ADF) software package,¹⁹ and validated on the solvation free energies and geometry optimization of a number of mono- to pentatomic neutral and charged species in aqueous solution¹⁷ and on conformational equilibria, tautomerization energies, and activation barriers of S_N2 reactions in various polar and nonpolar solvents.¹⁸

Recently, some of us applied radial, one-dimensional RISM theory of solvation using the OPLS classical force field to imidazolium-based ILs and found that it adequately describes the liquid structure²⁰ and solvation properties²¹ of these systems. In the present work, we employ the KS-DFT/3D-RISM-KH method as implemented in the ADF computational chemistry package¹⁷ to investigate the self-consistent electronic and classical solvation structure of ILs, which is feasible by using this methodology with a moderate amount of computing time.

2. Self-Consistent Field KS-DFT/3D-RISM-KH Method

The 3D molecular theory of solvation self-consistently coupled with Kohn–Sham DFT and CASSCF electronic structure theory has been comprehensively described in the literature,^{9,12,16–18} including the implementation and validation of KS-DFT/3D-RISM-KH with analytical gradients^{17,18} in the ADF computational chemistry software package¹⁹ we employed in this work. Below we only briefly summarize the method.

The electronic structure of the solute molecule is calculated from the KS-DFT equations modified to include the presence of solvent. The Helmholtz free energy of the whole system consisting of the solute and solvent is defined as

$$A[n_e(\mathbf{r}), \{\rho_\gamma(\mathbf{r})\}] = E_{\text{solute}}[n_e(\mathbf{r})] + \Delta G_{\text{solv}}[n_e(\mathbf{r}), \{\rho_\gamma(\mathbf{r})\}] \quad (1)$$

where E_{solute} is the electronic energy of the solute consisting of the standard components, ΔG_{solv} is the solvation free energy coming from the solute–solvent interaction and solvent reorganization in the presence of the solute molecule, $n_e(\mathbf{r})$ is the electron density distribution, and $\rho_\gamma(\mathbf{r})$ are the classical density distributions of interaction sites $\gamma = 1, \dots, s$ of solvent molecules. The solute energy is determined by the standard KS-DFT expression written in atomic units as

$$E_{\text{solute}}[n_e(\mathbf{r})] = T_s[n_e(\mathbf{r})] + \int d\mathbf{r} n_e(\mathbf{r}) v_i(\mathbf{r}) + \frac{1}{2} \int d\mathbf{r} d\mathbf{r}' \frac{n_e(\mathbf{r}) n_e(\mathbf{r}')}{|\mathbf{r} - \mathbf{r}'|} + E_{\text{xc}}[n_e(\mathbf{r})] \quad (2)$$

where $T_s[n_e(\mathbf{r})]$ is the kinetic energy of a noninteracting electron gas in its ground state with density distribution $n_e(\mathbf{r})$, $E_{\text{xc}}[n_e(\mathbf{r})]$ is the exchange–correlation energy, and $v_i(\mathbf{r})$ comprises the external potential and the nuclear attractive potential. Minimizing the free-energy functional (1),

$$\frac{\delta A[n_e(\mathbf{r}), \{\rho_\gamma(\mathbf{r})\}]}{\delta n_e(\mathbf{r})} = 0 \quad (3)$$

subject to the normalization condition for N_e valence electrons of the solute molecule,

$$\int d\mathbf{r} n_e(\mathbf{r}) = N_e \quad (4)$$

we obtain the self-consistent KS equation modified due to the presence of solvent,

$$\left(-\frac{1}{2}\Delta + v_i(\mathbf{r}) + v_h(\mathbf{r}) + v_{\text{xc}}(\mathbf{r}) + v_{\text{solv}}(\mathbf{r})\right)\psi_j(\mathbf{r}) = \varepsilon_j\psi_j(\mathbf{r}) \quad (5)$$

where the Hartree potential is

$$v_h(\mathbf{r}) = \int d\mathbf{r}' \frac{n_e(\mathbf{r}')}{|\mathbf{r} - \mathbf{r}'|} \quad (6)$$

the electron density distribution is determined by summation over the N_e lowest occupied eigenstates with account for their double occupancy by electrons with opposed spins

$$n_e(\mathbf{r}) = \sum_{j=1}^{N_e} |\psi_j(\mathbf{r})|^2 \quad (7)$$

the exchange–correlation potential is the functional derivative

$$v_{\text{xc}}(\mathbf{r}) = \frac{\delta E_{\text{xc}}[n_e(\mathbf{r})]}{\delta n_e(\mathbf{r})} \quad (8)$$

and the solvent potential is defined as

$$v_{\text{solv}}(\mathbf{r}) = \frac{\delta \Delta G_{\text{solv}}[n_e(\mathbf{r}), \{\rho_\gamma(\mathbf{r})\}]}{\delta n_e(\mathbf{r})} \quad (9)$$

The calculation of $v_h(\mathbf{r})$ in ADF is handled by using the fitted density

$$n_e(\mathbf{r}) \approx \sum_{j=1}^{N_e} c_a f_a(\mathbf{r}) \quad (10)$$

which after substitution to eq 6 yields the fitted potential expanded in terms of the single-center Slater functions f_a , with the coefficients c_a determined by least-squares fitting. (See also the citations in ref 17.) Together with using the locality properties, this allows one to dramatically reduce the amount of calculations necessary for evaluation of the potentials and matrix elements.

The total free energy is calculated as

$$A_{\text{tot}} = \sum_{j=1}^{N_e} \varepsilon_j - \frac{1}{2} \int d\mathbf{r} d\mathbf{r}' \frac{n_e(\mathbf{r}) n_e(\mathbf{r}')}{|\mathbf{r} - \mathbf{r}'|} + E_{\text{xc}}[n_e(\mathbf{r})] - \int d\mathbf{r} v_{\text{xc}}(\mathbf{r}) n_e(\mathbf{r}) + \Delta G_{\text{solv}}[n_e(\mathbf{r}), \{\rho_\gamma(\mathbf{r})\}] - \int d\mathbf{r} v_{\text{solv}}(\mathbf{r}) n_e(\mathbf{r}) \quad (11)$$

The classical density distributions of molecular solvent around a solute of arbitrary shape are obtained by solving the three-dimensional reference interaction site model (3D-RISM) integral equation

$$h_\gamma(\mathbf{r}) = \sum_\alpha \int d\mathbf{r}' c_\alpha(\mathbf{r}-\mathbf{r}') \chi_{\alpha\gamma}(r') \quad (12)$$

where $h_\alpha(r)$ and $c_\alpha(\mathbf{r})$ are respectively the 3D total and direct correlation functions of solvent site α around the solute macromolecule, and $\chi_{\alpha\gamma}(r)$ is the site–site susceptibility of pure solvent, the function determining a perturbation of bulk solvent in response to the potential of the solute macromolecule. It is expressed as

$$\chi_{\alpha\gamma}(r) = \omega_{\alpha\gamma}(r) + \rho_\alpha h_{\alpha\gamma}(r) \quad (13)$$

in terms of the intramolecular correlation function (or intramolecular matrix) $\omega_{\alpha\gamma}(r) = \delta(r - l_{\alpha\gamma})/(4\pi l_{\alpha\gamma}^2)$ specifying the geometry of a solvent molecule with site separations $l_{\alpha\gamma}$, and the intermolecular total correlation function $h_{\alpha\gamma}(r)$ of pure solvent with the number density ρ_α of solvent site α . The integral equation (12) must be complemented with a closure relating the total and direct correlation functions. The exact relation is a cumbersome functional of $h(r)$ and is replaced in practice with an approximation reflecting the physics of the system. The approximation proposed by Kovalenko and Hirata (KH closure)

$$g_\gamma(\mathbf{r}) = \begin{cases} \exp(-\beta u_\gamma(\mathbf{r}) + h_\gamma(\mathbf{r}) - c_\gamma(\mathbf{r})) & \text{for } g_\gamma(\mathbf{r}) \leq 1 \\ 1 - \beta u_\gamma(\mathbf{r}) + h_\gamma(\mathbf{r}) - c_\gamma(\mathbf{r}) & \text{for } g_\gamma(\mathbf{r}) > 1 \end{cases} \quad (14)$$

is a combination of the so-called hypernetted chain approximation (HNC) automatically applied to repulsive core regions of the distribution function and the mean-spherical approximation (MSA) for association peaks and attractive tails. It has been proven to be appropriate for various fluids with polar and/or charged associating species, and is particularly suitable for SCF coupling with an ab initio theory describing the solute macromolecule with a charge density distribution. The 3D-RISM-KH equations (12) and (14) lead to the solvation free energy in the closed analytical form

$$\Delta G_{\text{sol}} = \rho kT \sum_\gamma \int d\mathbf{r} \left[\frac{1}{2} (h_\gamma(\mathbf{r}))^2 \Theta(-h_\gamma(\mathbf{r})) - c_\gamma(\mathbf{r}) - \frac{1}{2} h_\gamma(\mathbf{r}) c_\gamma(\mathbf{r}) \right] \quad (15)$$

where Θ is the Heaviside step function. An important advantage is that the form (15) allows one to evaluate the functional derivative (9) analytically, and thus to obtain the SCF potentials coupling the electronic and classical subsystems as well as the analytical gradients of the solvation free energy with respect to solute nuclei geometry change. At present, to avoid cumbersome 6D quantum chemical calculation we model the dispersive part of the solute–solvent interaction potentials with the Lennard-Jones parametrization.

Before the self-consistent field calculations, the site–site radial correlation functions of bulk solvent $h_{\alpha\gamma}(r)$ are obtained from the dielectrically consistent RISM theory (DRISM) developed by Perkyns and Pettitt²² providing a consistent description of the dielectric properties for ions in polar solvent, which is complemented with the KH closure approximation to enable treatment of highly associating solvents.⁹

The long-range electrostatic part of all the correlation functions, both the 1D and 3D, is separated out and handled

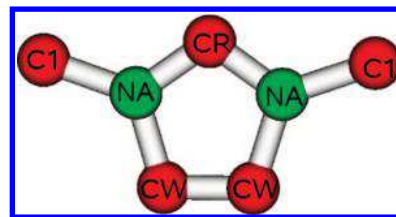


Figure 1. Ball-and-stick representation model of the [mmim] cation.

analytically. The remaining short-range parts of the 3D site correlation functions are specified on a 3D linear grid in a rectangular supercell (1D linear grid for the radial correlations), and the short-range part of the convolution in eq 12 is handled by using the 3D fast Fourier transform (3D-FFT) technique. For a macromolecular solute, the box size has to be large enough to ensure decay of the short-range part of the 3D site correlation functions at the supercell boundaries and absence of aliasing in convolution computation.

3. Models

In this paper, we investigate the behavior of the dimethylimidazolium chloride ([mmim][Cl]) ionic liquid. Figure 1 depicts the cation together with the atomic labels. This cation has been chosen for its simple molecular structure, which makes it an ideal model to theoretically investigate the behavior of ILs, and the simpler of these liquids ([mmim][Cl]), with a melting temperature of 390 K²³ has been used as a reference system for molecular dynamics simulation of ILs.^{24–29} In addition, its rigid structure in the absence of alkyl chains allows one to obtain the solvent intra- and intermolecular correlations (13) from RISM theory, which otherwise would require use of the polymer RISM approach.⁸

First, the DRISM-KH calculation for solvent structure at the classical level is performed as follows. The IL solvent is described as an equimolar mixture of the [mmim] cation and Cl anion at a temperature of 400 K and number density 0.00509 \AA^{-3} , with the [mmim] cation represented by the united-atom (UA) model treating the methyl groups and the CH units in the ring as single combined atoms. The interaction potential between interaction sites of species consists of the Coulomb term with the partial charges and the Lennard-Jones term with the size and energy parameters obtained from the standard Lorentz–Berthelot mixing rules. The UA2 force field parameters shown in Table 1 are taken from ref 30. Then, the solvent susceptibility $\chi_{\alpha\gamma}(r)$ is used as input to the KS-DFT/3D-RISM-KH equations. To achieve further self-consistency of the force field with the electronic structure calculation, the geometry and UA charges in the DRISM-KH calculation are set to the optimized geometry and the atomic charges derived from the electronic structure by using the multipole-derived charge analysis³¹ as implemented in ADF and iterated until self-consistency. Two independent calculation cycles were performed to get the self-consistency: one with multipole-derived charges at the dipole level (MDC-d) and the other at the quadrupole level (MDC-q). The charges obtained by this procedure, with the hydrogen charges included in these of the corresponding united atoms, are reported in Table 1.

The force field values obtained correspond to a rigid cation, as described in RISM theory with the intramolecular matrix $\omega_{\alpha\gamma}(r)$ corresponding to fixed bond lengths. However, recent simulation studies²⁶ showed that a considerable amount of polarization in ILs results from geometrical deformation of the cation, and the presence of flexible bonds and angles can

TABLE 1: Force Field Parameters for the [mmim] Cation in the UA2 Model and for the Cl Anion in the Description of the IL Solvent^a

species	atom	charge	charge (MDC-d)	charge (MDC-q)	ϵ_{ii} (kJ/mol)	σ_{ii} (Å)
[mmim]	CR	0.501	0.3606	0.4351	0.4359	3.880
	N	-0.267	-0.2750	-0.5667	0.6987	3.250
	CW	0.200	0.1729	0.2622	0.4359	3.880
	C1	0.316	0.4218	0.5880	0.8518	3.775
[Cl]	Cl	-1.000			0.4148	4.401

^a The [mmim] partial site charges are first taken from the force field and then self-consistently optimized at the MDC-d and MDC-q levels.

TABLE 2: All-Atom Force Field Parameters of the Lennard-Jones Potential Used in the 3D-RISM-KH Part of the SCF Procedure To Represent the Dispersion Interaction of the Solute Interaction Sites^a

atom	charge	ϵ_{ii} (kJ/mol)	σ_{ii} (Å)
CR	0.1520	0.2929	3.55
CW	0.0899	0.2929	3.55
C1	0.9810	0.2761	3.50
N	-0.5667	0.7112	3.25
HR	0.2831	0.1255	2.42
HW	0.1723	0.1255	2.42
H1	-0.1310	0.1924	2.50

^a Charges reported are those obtained from the MCD-q fitting procedure for each atom.

noticeably modify the effective partial charges of interaction sites in a force field for ILs. We will discuss this aspect later on. As described in our previous works,^{20,21} the radial RISM method is able to describe all the typical features of the IL structure: the alternating charge layering of cations and anions around each ionic species and the offset stacking interaction between imidazolium rings. In addition, the position of the peaks and the coordination numbers are in good agreement with the results obtained from MD simulation.²¹ The starting geometries of the cation and of the anions were obtained from quantum mechanics optimization in free space, and the IL density we used is taken from ref 26.

In the self-consistent field KS-DFT/3D-RISM-KH procedure, the KS-DFT calculations for the [mmim] cation solute were performed using the LDA exchange–correlation functional and the DZP basis set for all calculations. The 3D grid of 128³ nodes in a cubic box of size 64.0 Å was used for the 3D-RISM calculations. The all-atom (AA) force field parameters of the Lennard-Jones potential used in the 3D-RISM-KH part of the SCF procedure to represent the dispersion interaction of the solute interaction sites are given in Table 2.

4. Results

4.1. Radial Distributions, and Self-Consistent Charges and Geometry. We begin with the calculation of the self-consistent charges of the [mmim] cation, as described in the previous section. It is evident that the self-consistent charges of the [mmim] cation are quantitatively different from those from the classical force field, particularly for the quadrupole-level charges. Nevertheless, a comparison of the anion–cation radial distribution functions of the IL solvent obtained at the MDC-q and from the UA force field show little difference (Figure 2). The main effects of the self-consistent charges are the height change in the two peaks near the CR and CW sites and the slightly shifted position of the anion peak relative to the cation N atom. For the cation–cation distribution functions depicted in Figure 3 the use of the self-consistent MDC-q charges leads to an enhancement of the effective stacking between neighboring cations, as evident from the augmented

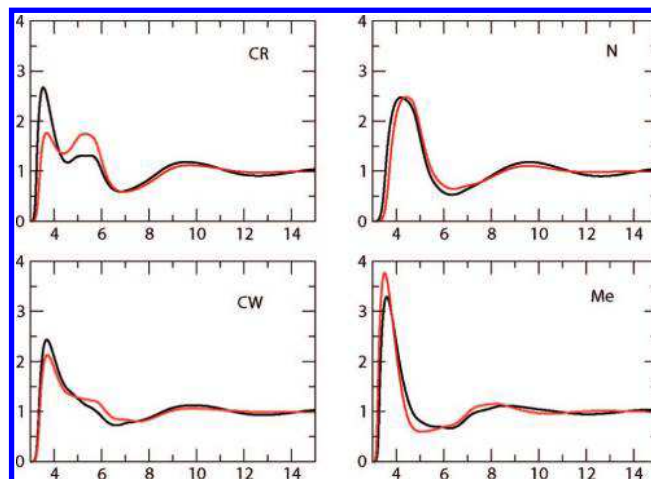


Figure 2. Radial distributions of the Cl anions with respect to the [mmim] cation sites (indicated in the upper right corner of each panel) in the IL. Results of the RISM-KH theory using the classical force field charges (black) and the self-consistent charges obtained at the MDC-q level (red).

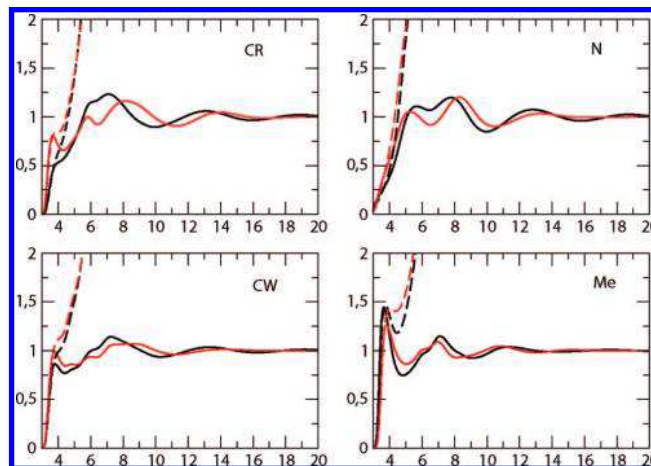


Figure 3. Radial distributions (solid lines) and running coordination numbers (dashed lines) between like sites of the [mmim] cation in the IL (site labels are indicated on each panel). Results of the RISM-KH theory using the classical force field charges (black) and the self-consistent charges MDC-q (red).

plots for the running coordination numbers (average number of sites within the given distance) at the distances larger than the peak at 4 Å corresponding to the stacking separation.

Even though the solvation structure of the IL does not change drastically upon the self-consistent charge and geometry optimization beyond the classical force field, it has to be recalled that the dynamics of melt is heavily affected by a choice of both charges³² and Lennard-Jones parameters.³³ Accurate determination of site charges, Lennard-Jones parameters and geometry is thus a key point in the development of a reliable force field for ionic liquids. Therefore, all the results presented

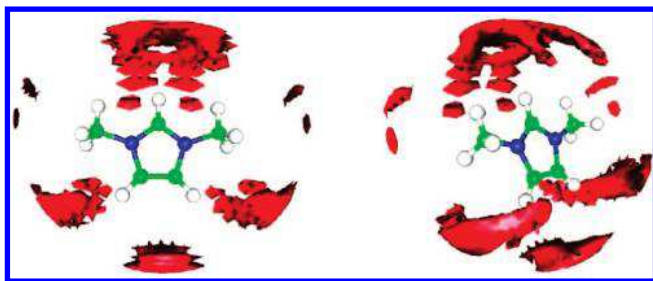


Figure 4. 3D distribution of the Cl anions around the [mmim] cation in the IL, predicted by the KS-DFT/3D-RISM-KH theory. Surfaces correspond to the probability density value 5.0 times larger than the bulk average density of the Cl anions.

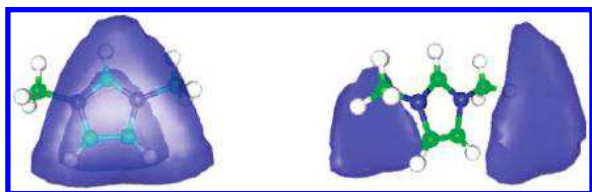


Figure 5. 3D distribution of the [mmim] cation nitrogen site around the whole [mmim] cation in the IL, predicted by the KS-DFT/3D-RISM-KH theory. Surfaces correspond to the probability density value 2.0 times larger than the bulk average density of the cation site.

below have been obtained with the self-consistent charges at the MDC-q level.

4.2. Three-Dimensional Distributions. First, we present the 3D distribution functions of the chloride anion around the imidazolium cation in the IL. As seen in Figures 4 and 5, the 3D distributions obtained are in good agreement with the conclusions obtained previously from classical MD or quantum-mechanical (SIESTA or CPMD) simulations. The Cl anion is located mainly around the ring hydrogens; it has to be noted that the correlation hole above the central ring hydrogen (which can be seen in classical simulations, but not in CPMD ones) is present in the distribution obtained by the KS-DFT/3D-RISM-KH method. This feature indicates that the hydrogen bonding between the Cl anion and the unique hydrogen is not reproduced by our calculations. No Cl anion appears to be coordinated to the methyl groups in the axial direction. The Cl anion distribution function assumes larger values above the unique ring hydrogen, compared to the twin hydrogens on the opposite side, which is in agreement with literature.^{24,28}

The cation distribution can be reconstructed by plotting the nitrogen spatial distribution; we see here that these sites are extremely strongly localized in the regions parallel to the ring plane. This is in agreement with recent *ab initio* simulations²⁸ showing that cations in the first coordination shell around the imidazolium cation are situated mainly in parallel to the neighboring rings. It appears from our calculations that the cations are located in a sort of antiparallel stacked arrangement, with the central hydrogens (CR) of neighboring sites pointing in the opposite directions. This is in agreement with the already observed augmentation of the stacking interaction in the MDC-q charge scheme described in the radial RISM calculations; in this last charge set, actually, the dipole moment along the CR-HR axis is augmented, and the dipole-dipole interaction is enhanced for the neighboring antiparallel dipoles. The radial distribution functions obtained by orientational averaging of the 3D distribution (Figure 6) show acceptable agreement, too. The cation-anion distribution exhibits a peak at 4.85 Å. The coordination number obtained by the integration up to 6.85 Å is 7.40; such findings are in agreement with the observation

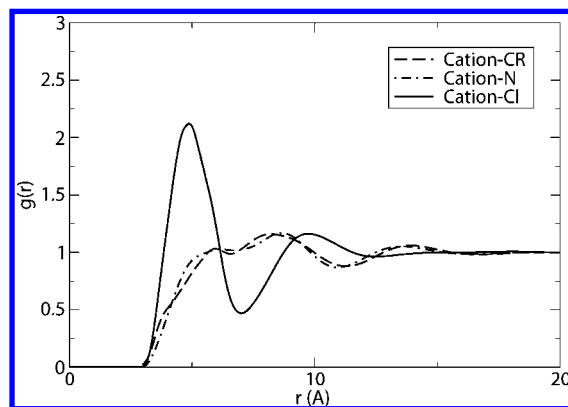


Figure 6. Radial distribution of the Cl anions (solid line), the cation CR site (dashed line), and the cation N site (dash-dotted line) around the center of mass of the [mmim] cation in the IL, obtained by orientational averaging of the 3D distributions from the KS-DFT/3D-RISM-KH theory.

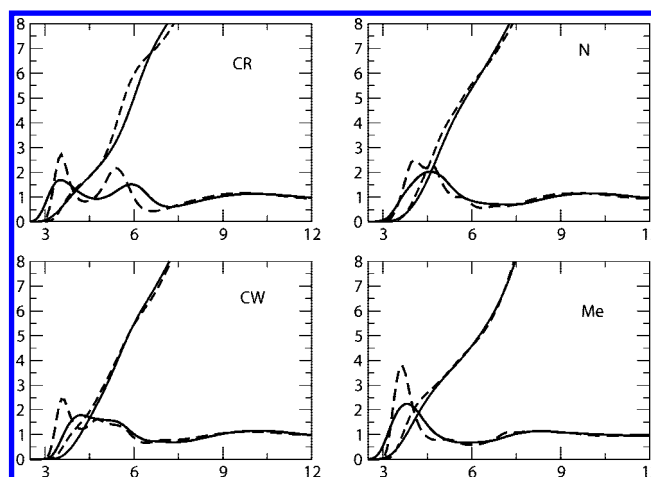


Figure 7. Radial distributions obtained by orientational average of the KS-DFT/3D-RISM-KH results with the self-consistent charges obtained at the MDC-q level (thick solid line), compared to the results of the classical MD simulation³⁸ (thick dashed line). The running coordination numbers corresponding to the above distributions are shown as well (thin lines).

made in the previous CPMD simulation²⁸ in which a coordination number of 7.5 for the anion around the cation was found.

The cation-cation distribution shows the expected alternating charge layering, with the stacking interaction evidenced from the first maxima for both the CR and N interaction sites of [mmim]; the parallelism between neighboring imidazolium ring planes is evidenced from the very similar behavior of the CR and N sites belonging to the same ring and displaying the first maximum at the same distance. However, these maxima are shifted with respect to those in the CPMD simulation by about 1 Å. The pair distribution functions between the chloride anion and the [mmim] cation sites are exhibited in Figure 7. The 3D distribution functions show a displacement of the peak maximum toward a larger value and a different peak height, compared to MD simulations, which, it must be recalled, are performed for a different (fixed charge) model. Nevertheless, the coordination numbers of the chloride anion are in good agreement with the MD simulations, and the general structure of the liquid appears to be well reproduced by the KS-DFT/3D-RISM-KH procedure.

The pair distribution functions between the chloride anion and the aromatic hydrogens of the [mmim] cation are presented in Figure 8. We note that the peak position is centered at about

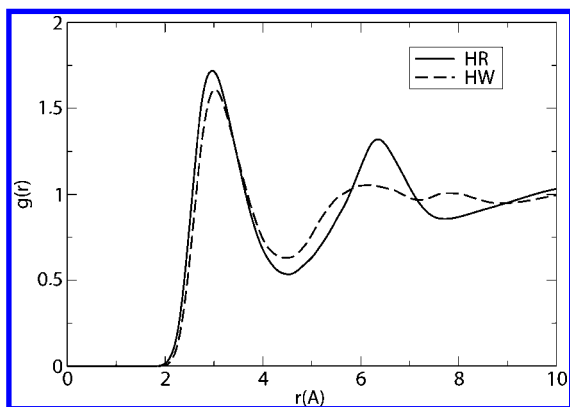


Figure 8. Radial distribution of the Cl anions around the aromatic hydrogens HR and HW (solid and dashed line, respectively) obtained by orientational averaging of the 3D distributions from the KS-DFT/3D-RISM-KH theory.

2.9 Å for HR and 3.01 Å for HW, in agreement with the classical MD simulation, whereas the CPMD simulation^{25,28} gives a H–Cl peak at 2.35 Å due to the formation of a hydrogen bond with the chloride anion. The higher coordination numbers we obtained (1.74 for HR, in contrast with 1.0 found in both the SIESTA and CPMD calculations) reflect an imperfect description of the hydrogen bond for the parameters chosen to perform our calculations. That can be further confirmed by noting that in our calculation the Cl density is localized mainly between the C–H bonds. As already observed,^{3,25} classical force fields tend to localize the maximum chloride density between C–H bonds, whereas *ab initio* calculations give the highest probability region above the ring hydrogens. In our 3D-RISM calculation, to describe the dispersion interactions, we used (for the solute cation) the classical LJ force field parameters due to Lopes et al.³⁴ The formation of hydrogen bonds between specific sites of the ionic liquids has probably to be resolved with a refinement of Lennard-Jones potential parameters between sites, eventually without recurring to mixing rules but specifically defining potential parameters between site pairs.

4.3. Dipole Moment. Next, we calculated the dipole moment of the [mmim] cation in the bulk and its polarization with respect to the gas phase. Recent Car–Parrinello simulation studies²⁶ showed that in the bulk phase the cation displays a considerable polarization induced by the localized coordination of counterions close to the ring hydrogens. The dipole moment value of a charged specie depends on the choice of axes origin: to compare our results with the ones cited above, we made the same choice of the origin, taken as the geometric center of the five ring atoms. The KS-DFT/3D-RISM-KH calculation confirms that in the bulk ionic liquid there is a considerable enhancement of the dipole moment of the cation due to polarization in the CR-H direction. We obtained a value of $\mu = 2.59$ D in the bulk IL, compared to $\mu = 2.10$ D for the isolated cation, which is in agreement with the values obtained in ref 26, $\mu = 2.67$ D in the IL vs $\mu = 2.11$ D for the isolated cation. Indeed, the difference is acceptable; a similar enhancement of the water dipole moment in liquid water calculated with Car–Parrinello MD gave values of 2.47 or 2.95 D, depending only on different partitioning schemes to attribute the density charge on the sites. (In CPMD, μ is calculated in an indirect manner, as the dipole of a classical charge distribution.) A calculation performed for a rigid [mmim] geometry of the solvated cation gave a dipole moment value of 2.48 D; this value indicates that the polarization is due to both the change in the electronic density and the geometry deformation of the cation, although the effect of the electronic

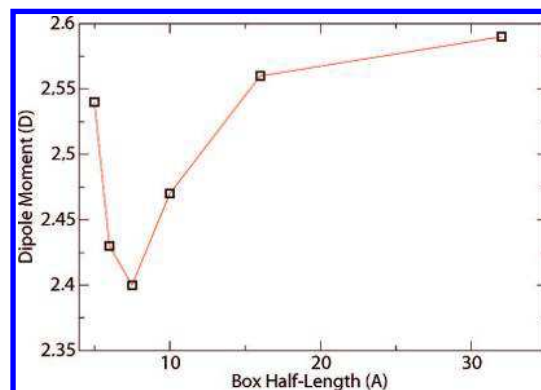


Figure 9. Dipole moment of the [mmim] cation in the IL as a function of the half-width of the calculation box, obtained from the KS-DFT/3D-RISM-KH theory.

polarization appears to be more significant, contributing about 80% of the effect.

The above difference of the dipole moment value from the CPMD results might be due to the imperfect description of the H–Cl hydrogen bond, described in the previous section. Another possible reason of the discrepancy is that the box size 11.6 Å containing 8 ionic pairs in the CPMD simulation²⁶ is insufficient to adequately represent the IL solvation structure, as all the essential features of the distribution functions should decay on the box half-width. Molten salt or ionic liquid are characterized with alternating shells of opposite screening charge with the Debye screening length λ_D that can be roughly estimated as the first peak separation for like ions (one screening shell);³⁵ for the [mmim][Cl] IL this amounts to $\lambda_D \approx 6$ Å, slightly exceeding the CPMD box half-width, not speaking of the next outer shells. To reveal the effect of (insufficient) box size, we performed several KS-DFT/3D-RISM-KH calculations for the [mmim] cation in the box of different width. As is evident from Figure 9, the box size has a significant effect on the dipole moment obtained: μ has a minimum when the box half-length is about the value of λ_D and levels up with the box size going well beyond λ_D .

4.4. Solvation Chemical Potential. Finally, we calculated the solvation free energy ΔG_{solv} of each of the two ions constituting the [mmim][Cl] IL, given in the KS-DFT/3D-RISM-KH method by the expression (15). We obtained a value of -22.14 kcal/mol for the [mmim] cation and -49.06 kcal/mol for the Cl anion, amounting in total to -71.20 kcal/mol for the [mmim][Cl] liquid. Even in the absence of direct experimental comparison for these numbers, we note that ΔG_{solv} has been indirectly estimated for ionic liquids to be about 70–100 kcal/mol.³⁶ The solvation free energy predicted by the KS-DFT/3D-RISM-KH theory appears then to be reasonable.

5. Conclusions

In this work, we adopted the KS-DFT/3D-RISM-KH method to study the solvation properties of room-temperature ionic liquid. The method predicts the IL properties in remarkable agreement with conclusions drawn from molecular dynamics simulations: the three-dimensional solvation structure is reproduced well, and the solvent environment effect of the constituents of the IL is described correctly. A minor drawback in the solvation structure obtained is the lack of hydrogen bonding between the chloride ion and the unique ring hydrogen (the actual presence of hydrogen bonding has been confirmed by NMR experiments combined with CPMD calculations);³ such a problem could probably be overcome by explicitly considering

coordinating anions described at a QM level around a cation. Another possible source of error is the use of the LDA functional; the need for gradient-corrected functionals on such calculations will be verified in future work.

The polarization due to the IL environment is found to be mainly due to electronic effects, in agreement with the previous studies. The possibility of accurate and computationally efficient self-consistent description of electronic structure and solvent environment in ILs opens up a wide range of possible applications the KS-DFT/3D-RISM-KH method to ab initio calculations for such systems. Here, we recall some of the most interesting examples. The first possible application could be a study of chemical reactions taking place in ionic liquids in which the solvent, beyond being the reaction media, plays a fundamental role as a coordinating agent.³⁷ Another fundamental issue is the structure of solutes in ionic liquids: because ILs take a major role in electrodeposition of transition metals, the structure and energetics of metal complexes as well as their solvation structure close to metal surfaces need to be studied thoroughly. Lastly, we point out that up to now the force fields used to simulate ionic liquids revealed considerable drawbacks, particularly in the reproduction of ion diffusive dynamics.³³ A possible pathway to refine these force fields is to perform accurate calculations for the effective interaction between ion pairs in solvent, rather than doing that in vacuo, until self-consistency is reached.

Acknowledgment. This work is supported by EC, Project FP6(STREP), Contract No. 517002 (IOLISURF). S.G. and A.K. acknowledge the support from the National Research Council (NRC) of Canada.

References and Notes

- (1) Welton, T.; Wasserscheid, P. *Ionic Liquids in Synthesis*; VCH-Wiley: Weinheim, 2007.
- (2) Bagno, A.; D'Amico, F.; Saielli, G. *J. Phys. Chem. B* **2006**, *110*, 23004.
- (3) Bagno, A.; D'Amico, F.; Saielli, G. *ChemPhysChem* **2007**, *8*, 873.
- (4) Wulf, A.; Fumino, K.; Michalik, D.; Ludwig, R. *ChemPhysChem* **2007**, *8*, 2265.
- (5) Chandler, D.; Andersen, H. C. *J. Chem. Phys.* **1972**, *57*, 1918–1930.
- (6) Hirata, F.; Pettit, B. M.; Rossky, P. J. *J. Chem. Phys.* **1982**, *77*, 509.
- (7) Hirata, F.; Rossky, P. J.; Pettit, B. M. *J. Chem. Phys.* **1983**, *78*, 4133.
- (8) Hansen J.-P.; McDonald, I. R. *Theory of Simple Liquids*, 3rd ed.; Academic Press: London, 1976; 316 pp.
- (9) *Molecular Theory of Solvation*; Hirata F., Ed.; Kluwer Academic Publishers: Dordrecht, The Netherlands, 2003; 360 pp.
- (10) Beglov, D.; Roux, B. *J. Phys. Chem.* **1997**, *101*, 7821.
- (11) Kovalenko, A.; Hirata, F. *Chem. Phys. Lett.* **2001**, *349*, 496.
- (12) Kovalenko, A.; Hirata, F. *J. Chem. Phys.* **1999**, *110*, 10095.
- (13) Moralez, J. G.; Ruez, J.; Yamazaki, T.; Motkuri, R. K.; Kovalenko, A.; Fenniri, H. *J. Am. Chem. Soc.* **2005**, *127*, 8307.
- (14) Tikhomirov, G.; Yamazaki, T.; Kovalenko, A.; Fenniri, H. *Langmuir* **2008**, *24*, 4447.
- (15) Johnson, R. S.; Yamazaki, T.; Kovalenko, A.; Fenniri, H. *J. Am. Chem. Soc.* **2007**, *129*, 5735.
- (16) Sato, H.; Kovalenko, A.; Hirata, F. *J. Chem. Phys.* **2000**, *112*, 9463.
- (17) Gusarov, S.; Ziegler, T.; Kovalenko, A. *J. Phys. Chem. A* **2006**, *110*, 6083.
- (18) Casanova, D.; Gusarov, S.; Kovalenko, A.; Ziegler, T. *J. Chem. Theory Comput.* **2007**, *3*, 458.
- (19) (a) te Velde, G.; Bickelhaupt, F.; van Gisbergen, S.; Guerra, C.; Baerends, E.; Snijders, J.; Ziegler, T. *J. Comput. Chem.* **2001**, *22*, 931. (b) Guerra, C.; Snijders, J.; te Velde, G.; Baerends, E. *Theor. Chem. Acc.* **1998**, *99*, 391. (c) ADF2004.01, SCM, Theoretical Chemistry, Vrije Universiteit, Amsterdam, The Netherlands, <http://www.scm.com>.
- (20) Malvaldi, M.; Bruzzone, S.; Chiappe, C. *Phys. Chem. Chem. Phys.* **2007**, *41*, 5576.
- (21) Bruzzone, S.; Malvaldi, M.; Chiappe, C. *J. Chem. Phys.* **2008**, *129*, 74509.
- (22) Perkyns, J. S.; Pettit, B. M. *J. Chem. Phys.* **1992**, *97*, 7656.
- (23) Zahn, S.; Uhlig, F.; Thar, J.; Spickermann, C.; Kirchner, B. *Angew. Chem., Int. Ed.* **2008**, *47*, 3639.
- (24) Hanke, C. G.; Price, S. L.; Lynden-Bell, R. M. *Mol. Phys.* **2001**, *99*, 801.
- (25) Del Pópolo, M. G.; Lynden-Bell, R. M.; Kohanoff, J. *J. Phys. Chem. B* **2005**, *109*, 5895.
- (26) Resende Prado, C. E.; Del Pópolo, M. G.; Youngs, T. G. A.; Kohanoff, J.; Lynden-Bell, R. M. *Mol. Phys.* **2006**, *104*, 2477.
- (27) Buhl, M.; Chaumont, A.; Schurhammer, R.; Wipff, G. *J. Phys. Chem. B* **2005**, *109*, 18591.
- (28) Bhargava, B. L.; Balasubramanian, S. *Chem. Phys. Lett.* **2006**, *417*, 486.
- (29) Krekeler, C.; Schmidt, J.; Zhao, Y. Y.; Qiao, B.; Berger, R.; Holm, C.; Delle Site, L. *J. Chem. Phys.* **2008**, *129*, 174503.
- (30) Lynden-Bell, R. M.; Atamas, N. A.; Vasilyuk, A.; Hanke, C. G. *Mol. Phys.* **2002**, *100*, 3225.
- (31) Swart, M.; van Duijnen, P.; Snijders, J. *J. Comput. Chem.* **1997**, *278*, 1068.
- (32) Yan, T.; Burnham, C. J.; Del Pópolo, M. G.; Voth, G. A. *J. Phys. Chem. B* **2004**, *108*, 11877.
- (33) Koddermann, T.; Ludwig, R.; Paschek, D. *ChemPhysChem* **2007**, *8*, 2464.
- (34) Lopes, J. N. C.; Deschamps, J.; Padua, A. A. H. *J. Phys. Chem. B* **2004**, *108*, 2038.
- (35) Del Pópolo, M. G.; Voth, G. A. *J. Phys. Chem. B* **2004**, *108*, 1744.
- (36) Krossing, I.; Slattery, J.; Daguene, C.; Dyson, P.; Oleinikova, A.; Weingärtner, H. *J. Am. Chem. Soc.* **2006**, *128*, 13427.
- (37) Acevedo, O.; Jorgensen, W.; Evanseck, J. *J. Chem. Theory Comput.* **2007**, *3*, 132.
- (38) Youngs, T. G. A.; Del Pópolo, M. G.; Kohanoff, J. *J. Phys. Chem. B* **2006**, *110*, 5697.

JP810887Z